Time Wells, Nested Basins, and Hyperknot Geometry

A Deepened Metric–Variational–Topological Theory of Proper Time

MineSpace.us

Abstract

We deepen an operational framework unifying gravitational and kinematic time dilation (proper time), the geometry of clock-rate fields (lapse N), basin and skeleton decompositions (Morse-like structure on Σ), and an explicit Hyperknot layer defined by weighted worldline communication graphs with stable invariants under deformation. We add: (i) rigorous redshift derivations via Killing energy and photon wavevector, (ii) explicit Euler–Lagrange derivation of geodesic extremization of proper time, (iii) static-Einstein relations linking N to curvature and matter (disciplining "time-well depth"), (iv) accelerated-frame/Rindler analysis explaining the twin paradox bookkeeping, (v) identifiability and gauge structure in inverse lapse reconstruction, and (vi) a concrete, multi-scale persistence signature for Hyperknot inference. A figure atlas provides diagrammatic anchors for each layer.

Contents

1 Executive Map and Notation

1.1 Four-layer stack

1. **Metric layer:** spacetime $(\mathcal{M}, g)$, causal structure, proper time τ.
2. **Clock-rate layer:** lapse N (static or a chosen slicing), redshift field.
3. **Basin layer:** gradient flow of N on (Σ, h), basins, separatrices, skeleton.
4. **Hyperknot layer:** worldline communication graph G with weights $(w_{ij}, \Delta t_{ij})$, filtered invariants and stability.

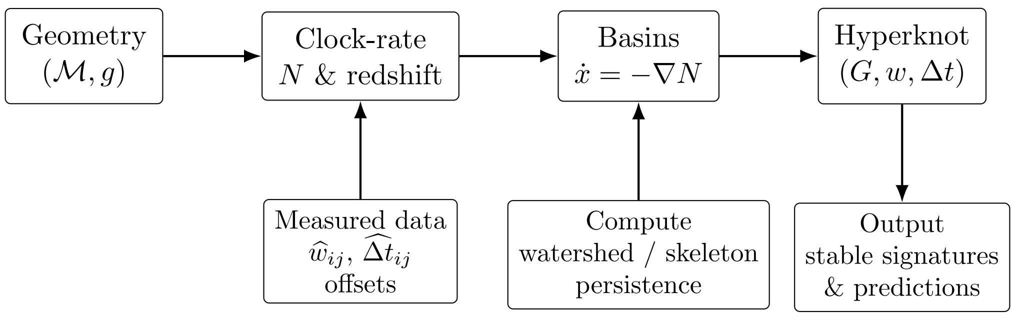

Figure 1: The pipeline: physics $\to$ lapse/redshift $\to$ basins $\to$ Hyperknot signatures.

1.2 Core warning about language

Remark 1.1 (Basins are classification, not a new force)**.** A "basin" is a partition of Σ induced by a scalar field (here N or $\log N$) and its gradient flow. This is not an additional physical interaction; it is a geometric decomposition of clock-rate structure already implied by $(\mathcal{M}, g)$.

2 Proper Time, Observers, and Photon Frequency

Definition 2.1 (Proper time)**.** For a future-directed timelike curve $\gamma(\lambda)$,

$$\tau[\gamma] = \int_{\lambda_0}^{\lambda_1} \sqrt{-g_{\mu\nu}(\gamma)\,\dot{\gamma}^\mu \dot{\gamma}^\nu}\ \mathrm{d}\lambda.$$

Definition 2.2 (Four-velocity)**.** An observer has four-velocity $u^\mu = \frac{dx^\mu}{d\tau}$ satisfying $g_{\mu\nu}u^\mu u^\nu = -1$.

Definition 2.3 (Observed photon frequency)**.** Let k^μ be the null wavevector of a light ray. The observed frequency by an observer u is

$$\nu = -\,u_\mu k^\mu.$$

2.1 Redshift as an invariant ratio

If emitter e and receiver r lie on the same null geodesic with wavevector k, then the frequency ratio is

$$\frac{\nu_r}{\nu_e} = \frac{(u \cdot k)_r}{(u \cdot k)_e}.$$

This is fully covariant and becomes concrete once the spacetime has symmetries (e.g., static Killing fields).

3 Static Spacetimes, Lapse Fields, and Exact Redshift Derivation

3.1 Static decomposition

Definition 3.1 (Static metric form)**.** A region is static if

$$ds^2 = -N(x)^2\, dt^2 + h_{ij}(x)\, dx^i dx^j,$$

with $N > 0$, $\partial_t g_{\mu\nu} = 0$, and vanishing shift in these coordinates.

Proposition 3.2 (Stationary clock rate)**.** *A stationary observer at fixed x measures*

$$d\tau = N(x)\, dt.$$

3.2 Killing energy and gravitational redshift

In a static spacetime, $\xi^\mu = (\partial_t)^\mu$ is a timelike Killing vector. Along any geodesic with tangent k^μ,

$$E := -\xi_\mu k^\mu$$

is conserved (Killing energy).

For a stationary observer, the four-velocity is $u^\mu = \xi^\mu/\sqrt{-\xi \cdot \xi}$. Since $-\xi \cdot \xi = N^2$, we have

$$u^\mu = \frac{\xi^\mu}{N}.$$

Then the measured frequency is

$$\nu = -u \cdot k = -\frac{\xi \cdot k}{N} = \frac{E}{N}.$$

Therefore:

Theorem 3.3 (Exact gravitational redshift for stationary observers)**.** *If the same photon is measured by stationary observers at x_1, x_2, then*

$$\frac{\nu_2}{\nu_1} = \frac{N(x_1)}{N(x_2)}.$$

Equivalently, clock-rate ratios satisfy $\frac{d\tau_1}{d\tau_2} = \frac{N(x_1)}{N(x_2)}$.

Remark 3.4 (Interpretation)**.** Deeper in a time well means smaller N, thus photons climbing out are redshifted and stationary clocks run slower relative to the same Killing time normalization.

3.3 ADM generalization and gauge

In a general $3+1$ split,

$$ds^2 = -N^2 dt^2 + h_{ij}(dx^i + \beta^i dt)(dx^j + \beta^j dt).$$

The lapse N depends on slicing choice; *ratios* inferred from physical redshift constraints are invariant once a stationary/Killing structure is fixed.

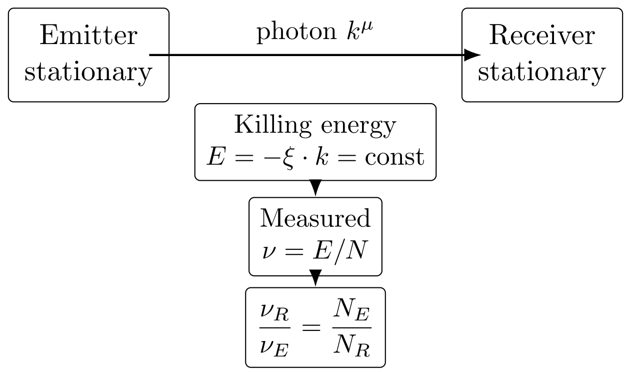

Figure 2: Exact static redshift derivation: conserved Killing energy implies $\nu = E/N$ for stationary observers.

4 Concrete Realizations: Schwarzschild, Weak Field, and SR+GR

4.1 Schwarzschild lapse

For a spherical mass M,

$$ds^2 = -\left(1 - \frac{2GM}{rc^2}\right) c^2 dt^2 + \left(1 - \frac{2GM}{rc^2}\right)^{-1} dr^2 + r^2 d\Omega^2,$$

$$N(r) = \sqrt{1 - \frac{2GM}{rc^2}} = \sqrt{1 - \frac{r_s}{r}}, \qquad r_s := \frac{2GM}{c^2}.$$

4.2 Weak-field potential

If $|\Phi|/c^2 \ll 1$,

$$g_{tt} \approx -\left(1 + \frac{2\Phi}{c^2}\right), \qquad N \approx 1 + \frac{\Phi}{c^2}.$$

4.3 Kinematic time dilation and combined first-order rate

For speed $v \ll c$,

$$\frac{\mathrm{d}\tau}{\mathrm{d}t} \approx 1 + \frac{\Phi}{c^2} - \frac{v^2}{2c^2}.$$

This is the standard first-order clock model used in high-precision timing networks.

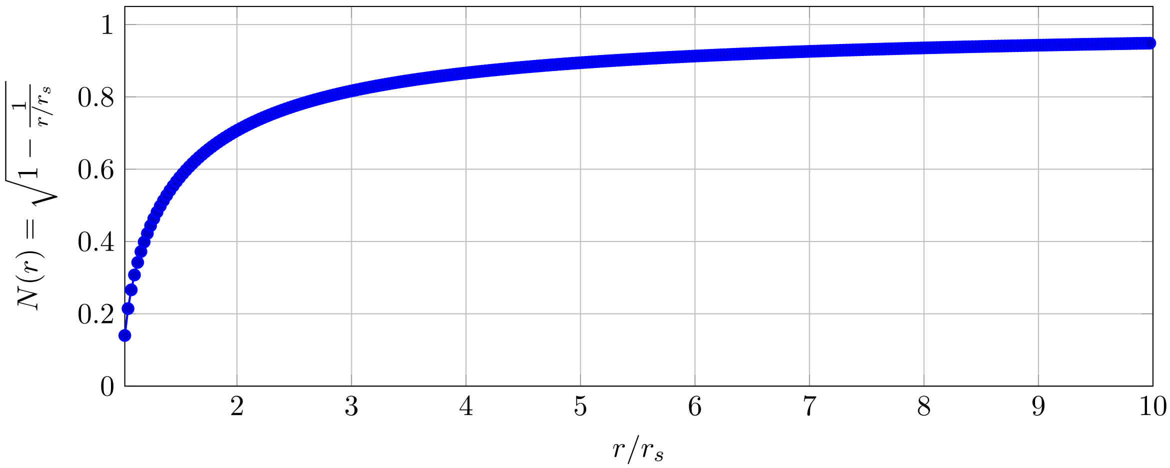

Figure 3: Schwarzschild time well: in static coordinates $N \to 0$ as $r \to r_s^+$.

5 Theorem I (Deepened): Basin Decomposition, Skeletons, and Stability

5.1 Gradient flow on (Σ, h)

Definition 5.1 (Gradient flow of the lapse)**.** On (Σ, h), define steepest descent

$$\frac{dx^i}{ds} = -h^{ij}\partial_j N.$$

Lemma 5.2 (Monotone descent of N)**.** *Along any flowline $x(s)$,*

$$\frac{\mathrm{d}}{\mathrm{d}s}N(x(s)) = -\,\partial_i N\, h^{ij}\partial_j N = -\,\|\nabla N\|_h^2 \le 0,$$

with equality iff $\nabla N = 0$.

Definition 5.3 (Time basin)**.** If $x_\star$ is a local minimum of N, define

$$\mathcal{B}(x_\star) = \{x \in \Sigma : \lim_{s\to\infty} \phi_s(x) = x_\star\}.$$

Theorem 5.4 (Basin partition (Morse-generic))**.** *If N is Morse-generic (non-degenerate critical points) and the flow is well-defined, then*

$$\Sigma \approx \bigsqcup_{x_\star \ \mathrm{min}} \mathcal{B}(x_\star)$$

up to boundaries formed by stable manifolds of saddles (measure zero in typical smooth settings).

5.2 Why $\log N$ is often the right scalar

Redshift constraints are multiplicative in N. Defining $f := \log N$ converts ratios into differences:

$$\log w_{ij} \approx f(x_j) - f(x_i).$$

Basins of f and N coincide (monotone transform), but $\log N$ has cleaner inference geometry.

5.3 Skeleton: separatrices as a topological carrier

Definition 5.5 (Separatrix set / skeleton)**.** Let $\mathcal{S} \subset \Sigma$ be the union of stable manifolds of saddles of N (or $f = \log N$). Then $\mathcal{S}$ forms the basin boundary complex. A discretization yields a graph/complex $\mathcal{K}$ we call the *basin skeleton.*

Proposition 5.6 (Stability away from bifurcations)**.** *If N is perturbed smoothly while remaining Morse-generic, then basin connectivity and skeleton homology are stable; changes occur only at degeneracy thresholds where critical points are created/annihilated.*

5.4 Algorithms (engineering detail)

Watershed (grid): $O(n)$ to label n cells using union-find or priority flood variants.
Critical-point skeleton (mesh): locate critical points, integrate separatrices; typically $O(n \log n)$ with adjacency queries and priority structures.
Robustness: smooth $f = \log N$ with a controlled kernel (or add Tikhonov/TV regularization) before skeleton extraction.

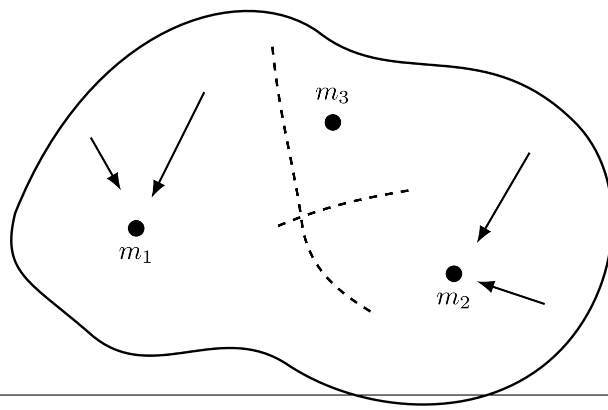

Basins of N (or $\log N$) from gradient flow.
Dashed curves are skeleton separatrices (stable manifolds of saddles).

Figure 4: Basin decomposition and skeleton: the geometric carrier of "time-well basins" on Σ.

6 Theorem II (Deepened): Proper-Time Extremization and the Twin Paradox

6.1 Euler–Lagrange derivation (explicit)

Let $L = \sqrt{-g_{\mu\nu}(x)\dot{x}^\mu \dot{x}^\nu}$. Vary $x^\mu(\lambda) \mapsto x^\mu + \varepsilon\eta^\mu$ with fixed endpoints. Standard calculus of variations yields

$$\frac{\mathrm{d}}{\mathrm{d}\lambda}\left(\frac{\partial L}{\partial \dot{x}^\alpha}\right) - \frac{\partial L}{\partial x^\alpha} = 0.$$

A convenient gauge is affine parameterization where L is constant; equivalently, one may extremize the equivalent functional

$$S[x] = \int \frac{1}{2}\, g_{\mu\nu}(x)\dot{x}^\mu \dot{x}^\nu \;\mathrm{d}\lambda$$

subject to timelike constraint. The Euler–Lagrange equations become the geodesic equation

$$\ddot{x}^\mu + \Gamma^\mu_{\alpha\beta}\dot{x}^\alpha \dot{x}^\beta = 0.$$

Theorem 6.1 (Geodesic extremization of proper time). *Between two timelike-separated events A, B in a convex normal neighborhood, the timelike geodesic extremizes proper time among nearby timelike curves with the same endpoints. In Minkowski spacetime, inertial worldlines locally maximize proper time.*

Corollary 6.2 (Twin paradox). *The traveling twin's worldline includes a non-inertial segment (frame change). For fixed endpoints A, B, the inertial worldline has maximal τ, hence the traveler returns younger.*

6.2 Simultaneity jump (the bookkeeping that resolves "reciprocity")

Set $c = 1$. Outbound Lorentz transform:

$$t' = \gamma(t - vx), \quad x' = \gamma(x - vt).$$

Inbound:

$$t'' = \gamma(t + vx), \quad x'' = \gamma(x + vt).$$

The slices $t' = \text{const}$ and $t'' = \text{const}$ tilt in opposite directions; switching frames at turnaround produces a discontinuous reassignment of which Earth event is "simultaneous" with the traveler.

6.3 Rindler bridge (acceleration as an effective gradient)

Uniform acceleration in Minkowski space can be described by Rindler coordinates (η, ρ) (in $1+1$D for clarity):

$$ds^2 = -(\rho a)^2 d\eta^2 + d\rho^2,$$

which has a lapse-like factor $N(\rho) = \rho a$. This exhibits a clock-rate gradient within the accelerated frame. It is not new physics; it is a coordinate manifestation consistent with the equivalence principle, useful for intuition during turnaround.

7 Theorem III (Deepened): Nested Basins, Scale Separation, and Discipline

7.1 Weak-field nesting via potential superposition

For weak fields,

$$\Phi_{\text{tot}} \approx \Phi_\oplus + \Phi_\odot + \Phi_{\text{MW}} + \cdots, \qquad \log N \approx \frac{\Phi_{\text{tot}}}{c^2}.$$

Proposition 7.1 (Dominant basin criterion). *If in a region U, $\|\nabla\Phi_A\| \gg \|\nabla\Phi_B\|$, then the gradient flow of $\log N$ is dominated by Φ_A in U, and the basin geometry at the scale of U is primarily determined by Φ_A.*

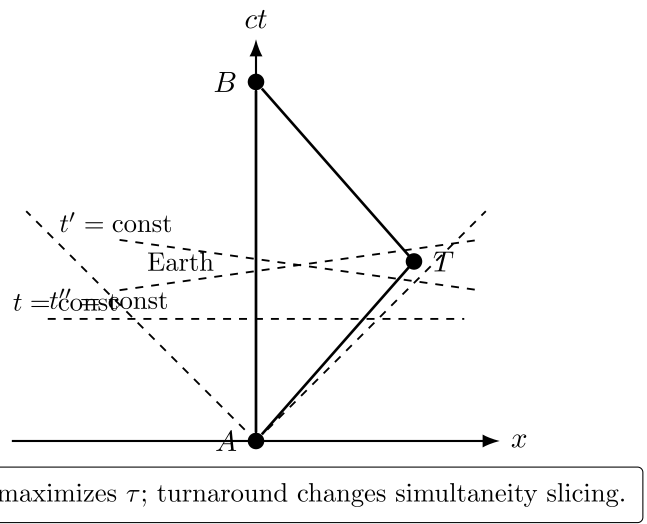

Figure 5: Twin paradox at maximum clarity: proper time differs by worldline; simultaneity is frame-dependent and jumps at turnaround.

7.2 Static Einstein discipline: how matter shapes N

In static vacuum, Φ obeys Laplace outside sources; more generally, Einstein's equations constrain the lapse and spatial curvature. A clean way to say "time wells come from mass-energy" is:

Remark 7.2 (Discipline statement)**.** In GR, the clock-rate geometry is not free; it is constrained by Einstein's equation $G_{\mu\nu} = 8\pi G T_{\mu\nu}/c^4$. In static settings, matter distributions source curvature and thereby constrain admissible lapse profiles. A "deeper well" is not a metaphysical claim; it corresponds to stronger curvature/matter content and boundary conditions.

7.3 Cosmological caution

Global notions of "largest basin" depend on slicing and boundary conditions. In FLRW cosmology, one uses cosmic time as a preferred foliation; the lapse can be set to 1 in comoving coordinates. Basin language is then local/relative rather than absolute.

8 Hyperknot Theory (Deepened): From Graphs to Cohomology-like Constraints

8.1 Worldline communication graph

Let $\mathcal{W} = \{\gamma_i\}$ be observer worldlines. Define a graph $G = (V, E)$, with an edge for each signal exchange. Weights:

$$w_{ij} := \frac{\nu_j}{\nu_i}, \qquad \Delta t_{ij}.$$

Definition 8.1 (Operational Hyperknot)**.** An operational Hyperknot is an equivalence class of weighted graphs $(G, w, \Delta t)$ under smooth metric deformations preserving (i) causal order and (ii) edge existence, up to measurement tolerance.

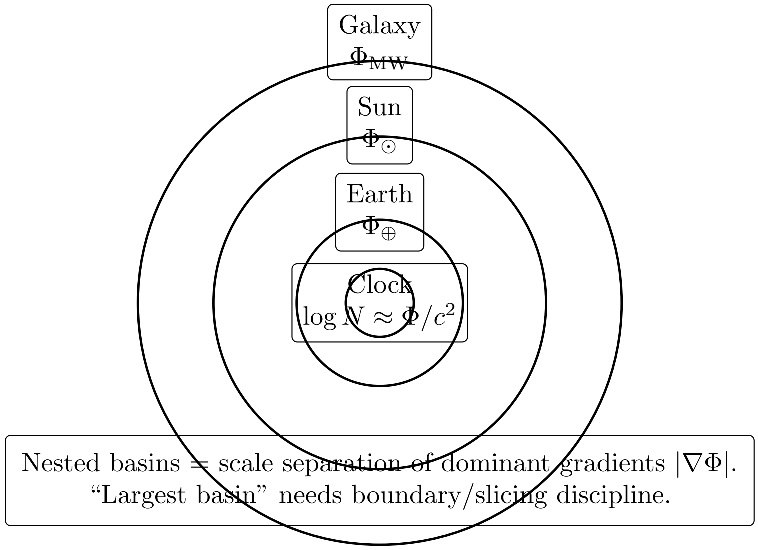

Figure 6: Nested time basins (conceptual) as dominance regimes of the lapse/potential gradient.

8.2 Additive potential and cycle-consistency

Define $f = \log N$. In static settings for stationary observers,

$$\log w_{ij} \approx f(x_j) - f(x_i).$$

This implies a *cycle consistency* condition: for any directed cycle C,

$$\sum_{(i\to j)\in C} \log w_{ij} \approx 0.$$

Deviations measure non-idealities: motion, non-stationarity, noise, or model mismatch.

Proposition 8.2 (Cycle residual as a diagnostic invariant)**.** *Define the cycle residual*

$$\mathcal{R}(C) := \left| \sum_{(i\to j)\in C} \log \widehat{w}_{ij} \right|.$$

In a static/stationary idealization, $\mathcal{R}(C) = 0$. Persistent nonzero $\mathcal{R}(C)$ across multiple cycles indicates either (a) kinematic contributions, (b) non-static geometry, or (c) systematic measurement bias.

8.3 Filtered topology (persistence signature)

Introduce a filtration parameter θ (e.g., keep edges with $\Delta t_{ij} \le \theta$ or $|\log w_{ij}| \le \theta$). As θ increases, the graph gains edges and cycles. Track:

- $\beta_0(\theta)$: connected components count (connectivity scale),
- $\beta_1(\theta)$: independent cycles count (loop complexity),
- distribution of cycle residuals $\mathcal{R}(C)$ across a chosen cycle basis.

These form a multi-scale Hyperknot signature.

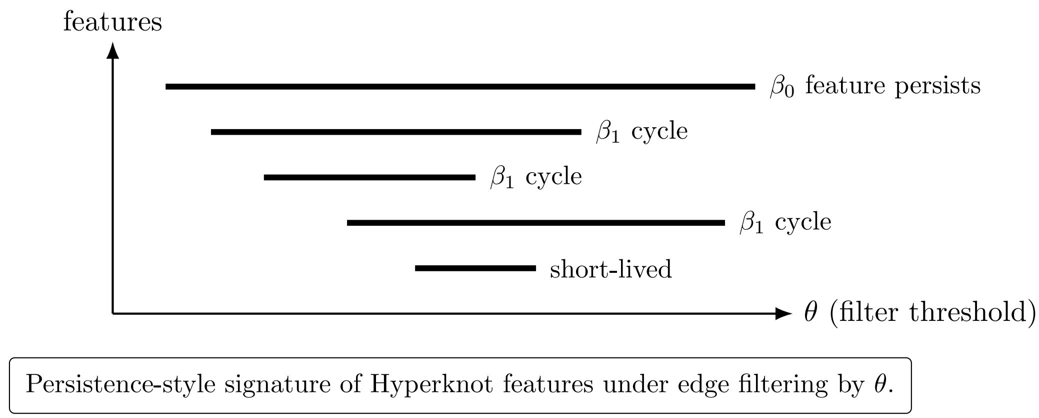

Figure 7: A persistence-style "barcode" schematic for multi-scale Hyperknot features. Long bars correspond to robust connectivity/cycle structure.

8.4 Figure: operational graph

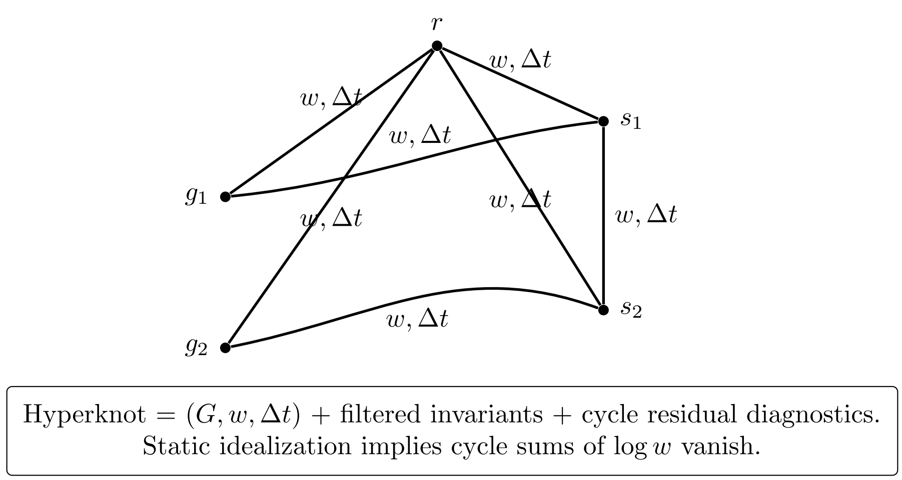

Figure 8: Operational Hyperknot graph: weights encode redshift and delay; topology encodes robust structure.

9 Inverse Problems (Deepened): Gauge, Identifiability, and Regularization

9.1 Gauge freedom (multiplicative)

Only ratios of N are directly observable in static/stationary redshift. Thus N is determined up to $N \mapsto \alpha N$ (global scale). Fix a reference x_0 with $N(x_0) = 1$, equivalently $f(x_0) = 0$ for $f = \log N$.

9.2 Graph-based reconstruction (additive form)

Let $\widehat{\ell}_{ij} := \log \widehat{w}_{ij}$. Model

$$\widehat{\ell}_{ij} \approx f(x_j) - f(x_i) + \epsilon_{ij}.$$

On a graph, this is a least-squares problem of the form $Af \approx \widehat{\ell}$, where A is an incidence matrix. Add smoothness on Σ:

$$\min_{f(\cdot)} \sum_{(i,j)\in E} \Big(\widehat{\ell}_{ij} - (f(x_j) - f(x_i))\Big)^2 + \lambda \int_{\Sigma} \|\nabla f\|_h^2 \, \mathrm{d}V_h.$$

Then reconstruct $N = \exp(f)$.

Remark 9.1 (Cycle residuals as quality control)**.** Because gradients are curl-free, large cycle residuals indicate either non-stationarity, kinematic motion, or systematic errors. This gives an intrinsic diagnostic for data integrity and model suitability.

10 A Concrete "Clock Array" Experiment (Expanded)

10.1 Objective

Recover a local approximation of $f = \log N$, segment basins, and extract a Hyperknot signature robust to noise.

10.2 Protocol

1. Deploy a reference clock at x_0 (fix gauge $f(x_0) = 0$).
2. Sample K additional clocks at x_k and measure $\widehat{w}_{ij}, \widehat{\Delta t}_{ij}$ on links.
3. Solve for $f(x_k)$ by graph least squares + smoothness prior (and optional outlier rejection using cycle residuals).
4. Interpolate f onto a grid/mesh; compute gradient flow; segment basins.
5. Construct filtration signatures of $G(\theta)$ and persistence of β_0, β_1; track cycle residual distributions.

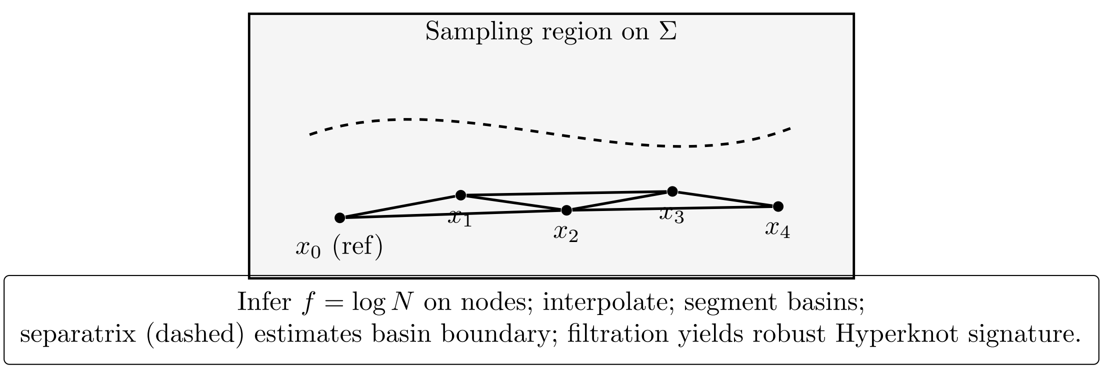

Figure 9: Clock array: a practical local reconstruction of time-well geometry and its robust signatures.

11 Entropy and Information Flow (Deeper Consequences)

11.1 Entropy bookkeeping across different proper times

Let S^μ be an entropy current with $\nabla_\mu S^\mu \geq 0$. For comoving entropy density s,

$$\frac{ds}{d\tau} \geq 0 \quad \Rightarrow \quad \frac{ds}{dt} = N(x)\frac{ds}{d\tau}.$$

This is a rescaling between coordinate-time accounting and local proper-time physics.

11.2 Information flow asymmetry

Because $\nu = E/N$ in static settings, photon energy/frequency changes with N. Combined with different proper-time sampling rates at endpoints, up/down links in a gravitational potential are intrinsically asymmetric in energetics and timing.

12 Disciplined Fixed-Point and "Largest Basin" Language

Definition 12.1 (Critical points of $f = \log N$)**.** A point $x_\star \in \Sigma$ is critical if $\nabla f(x_\star) = 0$. Minima correspond to well bottoms; saddles to basin boundaries; maxima to local peaks of clock rate.

Remark 12.2 (What a "fixed point" can mean operationally)**.** Operationally, "fixed point" should mean: a stable attractor of the gradient flow of f (a local minimum) *or* a stable feature of the basin skeleton under perturbations (a persistent node/cycle in the extracted complex). Anything beyond that requires additional dynamical hypotheses not present in GR.

Remark 12.3 (No new-force claim)**.** Basins classify scalar geometry of N (or $\log N$); Hyperknots classify stable global graph/skeleton structure. No extra physical force is introduced.

Closing Statement (Stronger)

Deep unified claim (GR-consistent): Proper time is the physical clock time along worldlines. In static regimes, the lapse N is the exact stationary clock-rate field, and redshift measurements determine N (up to gauge) through $\nu = E/N$. The spatial structure of N (or $f = \log N$) induces a basin decomposition by gradient flow, with a separatrix skeleton that is stable under small perturbations away from bifurcation thresholds. Independently, real clock networks define weighted worldline graphs $(G, w, \Delta t)$; in static/stationary idealizations, cycle sums of $\log w$ vanish, and filtered topological invariants provide robust multi-scale signatures (Hyperknot layer). The twin paradox is a direct consequence of proper-time extremization and simultaneity slicing changes at frame switches, with acceleration admitting an effective lapse gradient in Rindler coordinates. Together these components form a measurable, computable, and disciplined theory of "time wells" without introducing new forces.